Post-Hartree-Fock studies of the He/Mg(0001) interaction: Anti-corrugation, screening, and pairwise additivity

María Pilar de Lara-Castells', Ricardo Fernández-Perea, Fani Madzharova, and Elena Voloshina'

Citation: The Journal of Chemical Physics **144**, 244707 (2016); doi: 10.1063/1.4954772

View online: http://dx.doi.org/10.1063/1.4954772

View Table of Contents: http://aip.scitation.org/toc/jcp/144/24

Published by the American Institute of Physics

Post-Hartree-Fock studies of the He/Mg(0001) interaction: Anti-corrugation, screening, and pairwise additivity

María Pilar de Lara-Castells,[1,a)] Ricardo Fernández-Perea,[2] Fani Madzharova,[3] and Elena Voloshina[3,b)]
[1]*Instituto de Física Fundamental (CSIC), Serrano 123, E-28006 Madrid, Spain*
[2]*Instituto de Estructura de la Materia (CSIC), Serrano 123, E-28006 Madrid, Spain*
[3]*Humboldt-Universität zu Berlin, Institut für Chemie, Unter den Linden 6, 10099 Berlin, Germany*

(Received 4 April 2016; accepted 13 June 2016; published online 29 June 2016)

The adsorption of noble gases on metallic surfaces represents a paradigmatic case of van-der-Waals (vdW) interaction due to the role of screening effects on the corrugation of the interaction potential [J. L. F. Da Silva *et al.*, Phys. Rev. Lett. **90**, 066104 (2003)]. The extremely small adsorption energy of He atoms on the Mg(0001) surface (below 3 meV) and the delocalized nature and mobility of the surface electrons make the He/Mg(0001) system particularly challenging, even for state-of-the-art vdW-corrected density functional-based (vdW-DFT) approaches [M. P. de Lara-Castells *et al.*, J. Chem. Phys. **143**, 194701 (2015)]. In this work, we meet this challenge by applying two different procedures. First, the dispersion-corrected second-order Möller-Plesset perturbation theory (MP2C) approach is adopted, using bare metal clusters of increasing size. Second, the method of increments [H. Stoll, J. Chem. Phys. **97**, 8449 (1992)] is applied at coupled cluster singles and doubles and perturbative triples level, using embedded cluster models of the metal surface. Both approaches provide clear evidences of the anti-corrugation of the interaction potential: the He atom prefers on-top sites, instead of the expected hollow sites. This is interpreted as a signature of the screening of the He atom by the metal for the on-top configuration. The strong screening in the metal is clearly reflected in the relative contribution of successively deeper surface layers to the main dispersion contribution. Aimed to assist future dynamical simulations, a pairwise potential model for the He/surface interaction as a sum of effective He–Mg pair potentials is also presented, as an improvement of the approximation using isolated He–Mg pairs. *Published by AIP Publishing.* [http://dx.doi.org/10.1063/1.4954772]

I. INTRODUCTION

The interaction of noble-gas atoms with metal surfaces is relevant as a paradigmatic case of physisorption where interesting potential anti-corrugation effects can be revealed as the preferential adatom occupation of on-top sites instead of the expected hollow sites.[1] For example, different experimental measurements have proven the preferential Xe atom adsorption on the on-top positions of metallic surfaces.[2,3] Considering helium as the adsorbate, experimental evidences of anti-corrugation features were predicted by Annett and Haydock in the 1980s[4,5] and reported by Rieder *et al.* in the 1990s.[6] This behaviour was interpreted as the result of the hybridization of the occupied 1*s* He orbital with the unoccupied metal states;[4] an explanation which was, however, a matter of debate[7] and the possible role of the van-der-Waals (vdW) dispersion interaction in the potential anti-corrugation was also suggested.[7]

Anti-corrugation effects have been extensively analyzed in the repulsive interaction region through treatments based on density functional theory (DFT). Very recent advances to include the dispersion interaction has made possible to explore anti-corrugation effects in the vdW-dominated attractive region.[8,9] Thus, a preferential occupation of on-top sites for Xe atoms adsorbed on the Mg(0001) surface has been identified using a fully *ab initio* treatment.[8] This was explained as the result of screening effects for Xe atoms adsorbed on-top of Mg atoms, which are less likely when the adatom occupies the so-called "infinite-hollow" *fcc* sites.[10] Applying nonlocal vdW density functional theory,[11,12] opposite (corrugation and anti-corrugation) features have been reported for the Ne/Cu(111) and Xe/Cu(111) interaction potentials.[9] The different behaviour was explained by the weaker hybridization between the metal and the Ne orbitals. In this work, we analyze the He/Mg(0001) interaction. Due to the weak hybridization between 1*s* He orbitals and the $3s^{2-x}$ and $3p^{x}$ Mg states of the Mg(0001) surface, is not clear what the preferential adsorption site is, taking also into account the weakly bound nature and polarizability of the surface Mg 3*s* valence (free-like) electrons.

Between the different He-metal surface systems, the He/Mg(0001) system is particularly challenging due to the extremely small adsorption energy of He atoms (below 3 meV for a *fcc* Mg(111) surface[13,14]) and the strong delocalized nature and mobility of the surface electrons. The precise calculation of the He/Mg(0001) potential is now at reach for modern *ab initio* methodologies for intermolecular interactions as well as state-of-the-art vdW-

a)Author to whom correspondence should be addressed. Electronic mail: Pilar.deLara.Castells@csic.es
b)Electronic mail: elena.voloshina@hu-berlin.de

corrected DFT-based treatments (see, e.g., Ref. 15 and following articles). Furthermore, schemes combining fully *ab initio* and density functional theories have been recently proposed and successfully applied to the interaction of noble gases with non-metallic solid surfaces.[16–19] To study the He/Mg(0001) system, we have chosen two fully *ab initio* approaches instead. The first approach consists in applying the dispersion-corrected second-order Möller-Plesset perturbation theory (MP2C) of Heßelmann and Pitonák,[20,21] using bare (unembedded) surface cluster models of increasing size. This treatment replaces the uncoupled second-order dispersion contribution contained in the MP2 interaction energy with the coupled dispersion energy evaluated via time-dependent density functional response theory,[20] using the localized Hartree-Fock method.[22] The MP2C treatment has been successfully applied to numerous vdW-dominated adsorbate/surface interactions such as the interaction of atomic helium and Ag_2 with graphene.[23,24] The breakdown of the interaction energies has been also analyzed using DFT-based symmetry-adapted perturbation theory[25,26] [SAPT(DFT)].

The second approach consists in including the periodic boundary conditions at Hartree-Fock level while the coupled-cluster singles, doubles, and non-iterative triples [CCSD(T)] calculations are performed using the method of increments[27] and embedding cluster modelling. The method of increments was originally proposed by Stoll[27,28] and extensively applied by other groups to physisorption problems.[8,29–32] The localized orbitals are the essential building units making this method very efficient. The incremental approach is in general more difficult to apply when dealing with metal surfaces due to electronic delocalization effects. Voloshina, Gaston, and Paulus[33] developed a special embedding treatment to deal with this problem, and applied it to describe the Xe/Mg(0001) interaction,[8] among many other applications (see, for example, Ref. 34).

This work is also aimed to develop pairwise additive models capable of accounting for the strength and anisotropy of the interaction between He atoms and surfaces of condensed magnesium. This has been motivated by the development of the helium droplet-mediated (HDM) synthesis and deposition technique to create and gently deposit novel bimetallic nanoparticles/nanowires onto solid surfaces.[35–40] In particular, core-shell meta-stable pre-reactive cluster films of magnesium and different species have been recently created via the HDM experimental tool,[40,41] with promising applications in the area of chemical energy storage. In fact, previous experimental efforts have been conducted to form Mg nanoparticles to increase the surface/bulk ratio and to improve the efficiency of magnesium as a hydrogen storage material.[42,43] A basic understanding of the microscopic mechanisms behind these HDM processes makes it necessary to perform dynamical simulations relying on realistic interaction potentials. Ideally, these potentials are represented using pairwise additive models, beyond the sum of isolated He–Mg pair potentials. As a first step forward in improving this approximation, we present a pairwise potential model (PPM) which exploits the breakdown of the He/surface interaction energies in Hartree-Fock, and *intramonomer* and *intermonomer* correlation contributions.

The structure of this paper is as follows: Section II presents the structural models, the applied theoretical approaches and the computational details of the electronic structure calculations. The results obtained via the MP2C and SAPT(DFT) approaches and unembedded cluster models are discussed in Section III while those determined using the method of increments and embedded cluster models of the Mg(0001) surface are presented in Section IV. Finally, Section V describes our pairwise potential model while Section VI closes with the concluding remarks.

II. STRUCTURAL MODELS, THEORETICAL APPROACHES, AND COMPUTATIONAL DETAILS

A. Structural models

The structural models used in this work are illustrated in Figure 1. It shows the hexagonal close packed (*hcp*) crystalline structure of magnesium as well as the considered (unembedded) surface cluster models. The smallest cluster (Mg_{16}) includes the nearest and next-nearest neighbors to the central surface Mg atom, within the top-most layer, as well as the nearest Mg neighbors within the second layer. The largest cluster of composition Mg_{26} completes two hexagon-like shells around the central Mg atom within the surface plane, and adds next-nearest and nearest neighbors at the second and third layer, respectively. Our calculations considered both the "hollow" and "atop" adsorption positions shown in Figure 1.

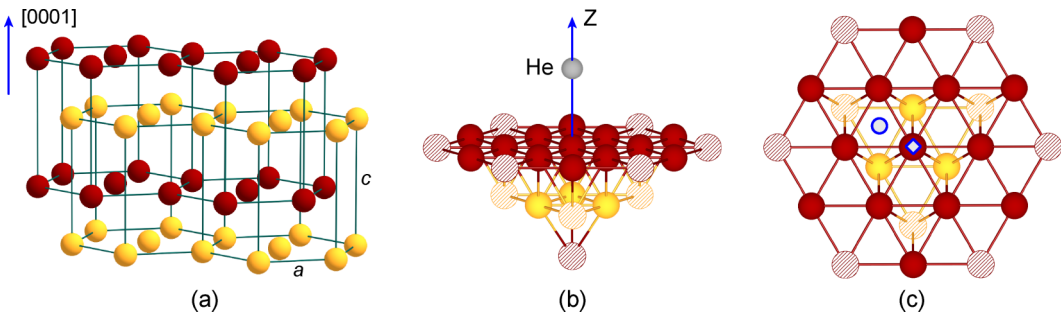

FIG. 1. (a) The hexagonal closed-packed structure of magnesium. The $ABAB\ldots$ sequence of layers is indicated with spheres of different [dark (red) and light (yellow)] colors. The lattice parameters a and c are indicated. (b) and (c) illustrate side and top view of the Mg(0001) surface fragments (Mg_{16} and Mg_{26}) chosen to perform the bare cluster calculations. Striped atoms are present only in the case of Mg_{26} cluster. The vertical distance of a helium atom above one magnesium atom (referred to as Z) is indicated in (b). Different adsorption positions of the helium atom are indicated in (c) with the rhombus and circle for the "atop" and "hollow" positions, respectively.

B. Theoretical approaches

1. Theoretical approaches applied to unembedded cluster models

The interaction energies between a helium atom and the bare (unembedded) cluster models shown in Figure 1 were obtained using two different approaches. First, supermolecular second-order Möller-Plesset (MP2) interaction energies ($E_{\rm int}^{\rm MP2}$) were calculated and corrected with the coupled MP2 (MP2C) treatment of Pitonák and Heßelmann.[20,21] In this way, uncoupled MP2 dispersion contributions ($E_{\rm disp}^{\rm UCHF}$) are replaced with those obtained via time-dependent density functional (TDDFT) response theory ($E_{\rm disp}^{\rm TDDFT}$).[20] The total interaction energy $E_{\rm int}^{\rm total}$ is thus determined as

$$E_{\rm int}^{\rm total} = E_{\rm int}^{\rm MP2} - E_{\rm UCHF}^{\rm disp} + E_{\rm TDDFT}^{\rm disp}. \quad (1)$$

The necessary Kohn-Sham orbitals and orbital energies were calculated using the localized Hartree-Fock method by Della Sala and Görling.[22]

Along with the MP2C approach, He/cluster interaction energies were calculated using the SAPT(DFT) method.[25,26] This method decomposes the interaction energy as a sum of first- and second-order interaction terms, namely, first-order electrostatic $E_{\rm elec}$ and exchange $E_{\rm exch}$, second-order induction $E_{\rm ind}$ and dispersion $E_{\rm disp}$ terms, along with their respective exchange corrections ($E_{\rm exch-ind}$ and $E_{\rm exch-disp}$). The δ(HF) estimate[44,45] of the higher-order induction plus exchange-induction contributions was added to the interaction energies. The total dispersion energy was obtained as the sum of dispersion and exchange-dispersion contributions. Similarly, the total induction energy was evaluated by adding the induction, exchange-induction and δ(HF) terms. We used the Perdew-Burke-Ernzerhof (PBE) density functional[46] and, then, the treatment will be referred to as SAPT(PBE).

2. The method of increments using embedding cluster modeling

The application of the method of increments to atoms physisorbed on a metal surface has been extensively described in Ref. 8, to which the interested reader is referred. Very briefly, the total interaction energy $E_{\rm int}^{\rm total}$ is first partitioned into Hartree-Fock (HF) $E_{\rm int}^{\rm HF}$ along with *intermonomer* and *intramonomer* correlation contributions ($E_{\rm int}^{inter}$ and $E_{\rm int}^{intra}$),

$$E_{\rm int}^{\rm total} = E_{\rm int}^{\rm HF} + E_{\rm int}^{intra} + E_{\rm int}^{inter}. \quad (2)$$

For vdW-dominated interactions, the *intermonomer* correlation term can be identified with the main dispersion contribution.[19] Within the method of increments, the Hartree-Fock contribution is calculated using a periodic surface model (see Sec. II C 3). The correlation calculations are performed for finite embedded fragments, reflecting the lattice structure of the system under study (here: Mg(0001) with He atoms occupying either "atop" or "hollow" adsorption sites). The total correlation energy is written as a cumulant expansion in terms of contributions from localized orbital groups (LOGs) of increasing size centered at the adsorbate (A) and atoms of the substrate (i, j, ...). The *intermonomer* correlation term $E_{\rm int}^{inter}$ is expressed as

$$E_{\rm int}^{inter} = \sum_i \eta_{Ai} + \sum_{i<j} \eta_{Aij} + \cdots, \quad (3)$$

where the two-body η_{Ai} increments are defined as the non-additive portion of the correlation energy $\Delta\varepsilon_{Ai}$ obtained when the electrons occupying the LOGs centered at the He and the i atom are simultaneously correlated, via excitations into the available virtual orbitals, $\eta_{Ai} = \varepsilon_{Ai} - \varepsilon_A - \varepsilon_i$. The third-order incremental terms (η_{Aij}) are defined analogously.[27] The *intramonomer* correlation term is calculated as

$$E_{\rm int}^{intra} = \eta_A + \sum_i \eta_i + \sum_{i<j} \eta_{ij} + \cdots, \quad (4)$$

where η_A is the correlation contribution to the adsorption energy within the adsorbate, and η_i and η_{ij} are one- and two-body contributions accounting for modifications in the surface increments due to the adsorption of the He atom. As previously discussed, for He/surface interactions (see, e.g., Ref. 17), four- and higher-order incremental contributions can be typically ignored. We notice that the embedded cluster model depends on the particular increment to be calculated. For example, Figure 2 shows the cluster used to calculate the correlation energy increments (η_{Ai}, η_{Aji}, η_{ij}) involving two Mg atoms which are nearest and next-nearest neighbors to the adsorbate, when located at the "atop" position. Besides the Hartree-Fock method, the vdW-corrected PBE-D2 approach of Grimme and collaborators[47] has been also applied using a periodic model of the Mg(0001) surface.

C. Computational details

1. MP2C and SAPT(DFT) cluster calculations

In all surface cluster calculations, correlation consistent basis sets were employed using the MOLPRO package.[48] The augmented polarized correlation-consistent triple-ζ basis of Woon and Dunning, Jr.[49] (aug-cc-pVTZ) was adopted for the cluster Mg atoms. The SAPT(PBE) calculations were

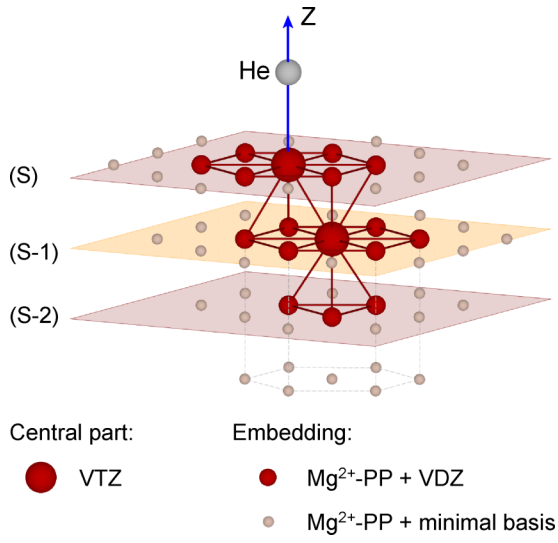

FIG. 2. Example of a cluster used in the incremental calculations. Spheres of different sizes represent atoms of different types.

performed using the aug-cc-pV5Z and aug-cc-pVTZ basis sets for He and Mg atoms, respectively. As presented below, test calculations showed that the enlargement of the He basis set from aug-cc-pVTZ to aug-cc-pV5Z, increases the well-depth by less than 0.12 meV (ca. 9%). Uncontracted aug-cc-pVTZ basis sets were used in the cluster (frozen-core) MP2C calculations for both Mg and He atoms. It was found that the enlargement of the He basis set to the uncontracted aug-cc-pVQZ basis increases the He/Mg_{16} well-depth for both "atop" and "hollow" structures by less than 0.1 meV (ca. 3%). The uncontracted Mg basis set was enhanced with additional tight p, d, and f primitive functions from the cc-pCVTZ basis set[50] to recover attractive core-correlation (CV) effects. The CV contribution was estimated via MP2C calculations in which the core Mg electrons were correlated, using a Mg_7 cluster composed by the central atom shown in Fig. 1 and its nearest neighbors. The CV contribution as a function of the He-surface distance was added to the MP2C interaction energies calculated for the He/Mg_{16} and He/Mg_{26} systems.

The performance of the MP2C method to describe the He–Mg interaction has been analyzed by determining the interaction potential and comparing it with that reported by Hinde,[51] employing basis sets near the complete basis set limit (CBS) and the CCSDT approach (see the supplementary material[64]). The largest relative deviation at the potential minimum is 0.08 meV (ca. 14%), reducing to 0.01 meV when accounting for basis-set incompleteness (BIC) in the MP2C calculations. The He–Mg interaction energy was also calculated at CCSDTQ level using the Kallay's MRCC program[52,53] interfaced to the MOLPRO package[48] (i.e., including fully triple T and quadruple Q excitations). The MP2C and CCSDTQ interaction energies agreed to within 0.01 meV and 1.5% (see Figure S1 of the supplementary material[64]). As a further validation test, additional CCSD(T) calculations were carried out for the He/Mg_7 system. Using the aug-cc-pVTZ basis, MP2C interaction energies deviated by less than 0.2 meV (ca. 7%) from those determined at CCSD(T) level.[64]

In the SAPT(PBE) calculations, the exchange-correlation PBE potential was asymptotically corrected[54] with the ionization potential value reported in the NIST Chemistry Web Book for atomic helium[55] and Hartree-Fock values for the bare Mg_n clusters. A spatial grid in between 3.2 and 10 Å was considered (about 13 values of the Z distance). The complete basis set (CBS) limit at the equilibrium of the "atop" and "hollow" He/Mg_{16} structures was estimated using the aug-cc-pVTZ and aug-cc-pVQZ basis sets. Specifically, the correlation energies evaluated at SAPT(DFT) level were extrapolated using the n^{-3} scheme of Helgaker and co-workers[56] with n = 3 and 4,

$$E_n^{corr} = E_{CBS}^{corr} + A\, n^{-3}.$$

The extrapolated CBS estimations of the correlation energies E_{CBS}^{corr} were added to the HF energies obtained with the aug-cc-pVQZ basis set. This procedure was extended to the MP2C interaction energies, as determined for "atop" and "hollow" He/Mg_7 structures in the relevant range of intermonomer distances by using uncontracted aug-cc-pVTZ and aug-cc-pVQZ basis sets. Next, CBS-accounting upscaling factors f_{CBS} were calculated as the ratio between the E_{CBS}^{corr} values and those determined using the aug-cc-pVTZ basis, attaining a weak Z-dependence. Finally, the MP2C He/Mg_n interaction energies with n = 16 and 26 were rescaled with the largest f_{CBS} values (ca. 1.04), obtaining an estimate of CBS-corrected PECs. All interaction energies presented in this work are counterpoise-corrected.[57]

2. Cluster calculations with the incremental approach

The method of increments was applied using the CCSD(T) approach, following the same computational setup reported in Ref. 8. The convergence of the perturbative expansion was assessed by quantifying the weight of perturbative triples (T) contributions, being as high as 10%–11% at the shortest Mg-Mg distance and decaying as it increases. In addition to pointing out a minor role of quadruple excitations, this validates the adequacy of a single-reference correlation treatment for the He/Mg(0001) interaction. The aug-cc-pVTZ and cc-pVTZ basis sets were used for He and central Mg atoms (see Fig. 2). As indicated in Fig. 2, the embedding Mg atoms within the first shell were described with a two-valence electron pseudopotential[58] (referred to as Mg^{2+}-PP+VDZ), while a minimal basis set was used for the embedding Mg atoms contained in the second solvation shell. The occupied orbitals of the embedding Mg atoms are not correlated (see Refs. 8 and 33 for the details of the embedding approach). As specified in Ref. 8, the distance between Mg atoms was varied up to 7.85 Å.

3. Periodic calculations

The CRYSTAL09 and CRYSTAL14 codes[59,60] were used for the periodic Hartree-Fock and PBE calculations, respectively. These calculations were realized following the computational setup reported in Ref. 8 for the Xe/Mg(0001) system, using the aug-cc-pVTZ basis set for He. The Mg(0001) surface was modeled with a nine-layer slab, considering both (2 × 2) and (3 × 3) supercells. The interaction energies using the (2 × 2) model differed from those evaluated using the (3 × 3) supercell by less than 11% (6% at the global potential minimum). The lattice parameters were fixed to the values of a = 3.2089 Å and c = 5.2102 Å. Structural relaxation effects of the magnesium atom positions were not included. We considered the "atop" and "hollow" adsorption sites shown in Figure 1 and a Z grid ranging from 3.5 to 8 Å.

III. ANALYSIS OF THE HE/SURFACE INTERACTION VIA THE SAPT(PBE) AND MP2C APPROACHES

A. Analysis of the He/surface interaction via the SAPT(PBE) approach

The He-metal interaction is an interesting case to be explored via the SAPT(DFT) method because it decomposes the interaction energy in physical meaningful contributions. For this purpose, the surface has been modeled with the Mg_{16} cluster shown in Figure 1. Figure 3 plots the individual energy contributions as a function of the He-cluster separation while

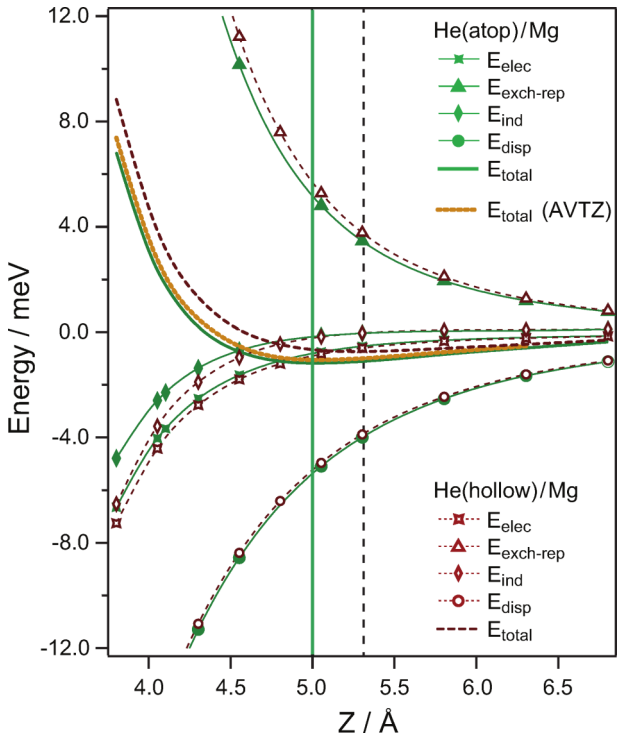

FIG. 3. SAPT(PBE) decomposition of the He/Mg_{16} interaction energy as a function of the He–Mg_{16} distance (see also Table I). Dashed and solid lines correspond to the adsorption of the He atom at "atop" and "hollow" surface sites (see Figure 1). The vertical green and dashed lines indicate the potential minimum positions for "atop" and "hollow" configurations, respectively. They have been determined by cubic spline interpolation of the total interaction energies.

Table I lists the values of the individual energy contributions for the potential minima at "atop" and "hollow" adsorption sites.

The vdW interaction essentially results from the balance of the exchange-repulsion and the attractive dispersion interaction (notice the small magnitude of the induction contribution). The electrostatic component is also attractive and its weight to the total attractive term is about 13% and 14% at the potential minima for "atop" and "hollow" configurations, respectively (see Table I). Notice that the binding energy is very small (below −1.4 meV). Figure 1 also shows the PEC determined with the aug-cc-pVTZ basis for the He atom at the "atop" configuration. CBS estimations of the well-depth values are presented in Table I. These values

TABLE I. SAPT-based decomposition of the He/Mg_{16} interaction energy at the equilibrium distances for "atop" and "hollow" configurations shown in Figure 1 (see also Figure 3).

	"atop"	"hollow"
Z_e/Å	5.0	5.3
E_{elec}/meV	−0.81	−0.65
$E_{exch-rep}$/meV	5.16	3.79
E_{ind}/meV	−0.19	0.01
E_{disp}/meV	−5.37	−3.88
E_{total}/meV	−1.21	−0.73
E_{total} (estimated CBS)/meV	−1.37	−0.88

are converged to within 0.16 and 0.15 meV for "atop" and "hollow" structures (ca. 12%-17%).

As can be seen in Figure 3 and Table I, the SAPT(PBE) approach predicts the "atop" site as the most stable position for the He/Mg_{16} interaction. The preferential binding at the "atop" site is mostly determined by the smaller Pauli exchange-repulsion (see Table I), allowing for a closer approximation of the He atom to the Mg_{16} cluster. This is reflected in the shorter equilibrium distance for the "atop" configuration (5.0 vs. 5.3 Å, see Figure 3). As a result, at the potential minima, both the dispersion and electrostatic terms are a factor of 1.4 and 1.2 more attractive for the "atop" geometry (see Table I). The third feature to note is that the attractive induction energy for the "atop" configuration (−0.19 meV, see Table I) accounts significantly for the difference between the well-depths (−0.48 meV). It might reflect the distortion of the bare Mg_{16} cluster to accommodate the electronic density provided by the adatom. This distortion is less feasible when the He adatom occupies the "hollow" site so that the induction energy bears a negligible value for this configuration (0.01 meV, see Table I).

B. Analysis of the He/surface interaction via the MP2C approach

Physical insights into the fundamental reasons why the "atop" site is more attractive (i.e., the anti-corrugation nature), are provided by applying the MP2C approach to the He/Mg_{16} and He/Mg_{26} systems. Figure 4 shows the total and individual energy contributions to the interaction as a function of the Z distance (see Eq. (1)) while Table II lists the values for these contributions at the potential energy minima.

Notice that the anti-corrugation, defined as the difference between the well-depths of the "atop" and "hollow" potentials, is enhanced upon increasing the cluster size (see the upper-left panel of Figure 4). Whatever the cluster size, the net repulsive contribution rises exponentially but less steeply for the "atop" configuration so that the equilibrium distance (Z_e) is shorter for this geometry (see Table II). This is the reason why the dispersion energies E^{disp}_{TDDFT} are significantly more attractive at the "atop" potential minima (see Table II). When modeling the surface with the Mg_{16} cluster, the Hartree-Fock contribution is less repulsive for the "atop" configuration (see the upper-right panel of Figure 4) while the remaining correlation contributions are almost identical (see the lower-left panel of Figure 4). In short, the site preference is not determined by electron correlation effects. Importantly, the opposite holds for the He/Mg_{26} system: the HF interaction energies are indeed more repulsive for the "atop" configuration (see the upper-right panel of Figure 4), as would have been expected from steric considerations. As can be seen in the lower-left panel of Figure 4 (green line), the correlation term ($E^{tot}_{int} - E^{HF}_{int} - E^{disp}_{TDDFT}$) becomes attractive at short distances when the He atom locates on-top of the central Mg atom, making the net repulsive contribution smaller despite of the larger (more repulsive) Hartree-Fock contribution.

Since the main dispersion contribution is subtracted, the magnitude ($E^{tot}_{int} - E^{HF}_{int} - E^{disp}_{TDDFT}$) could tentatively be associated with an *intramonomer* correlation contribution.

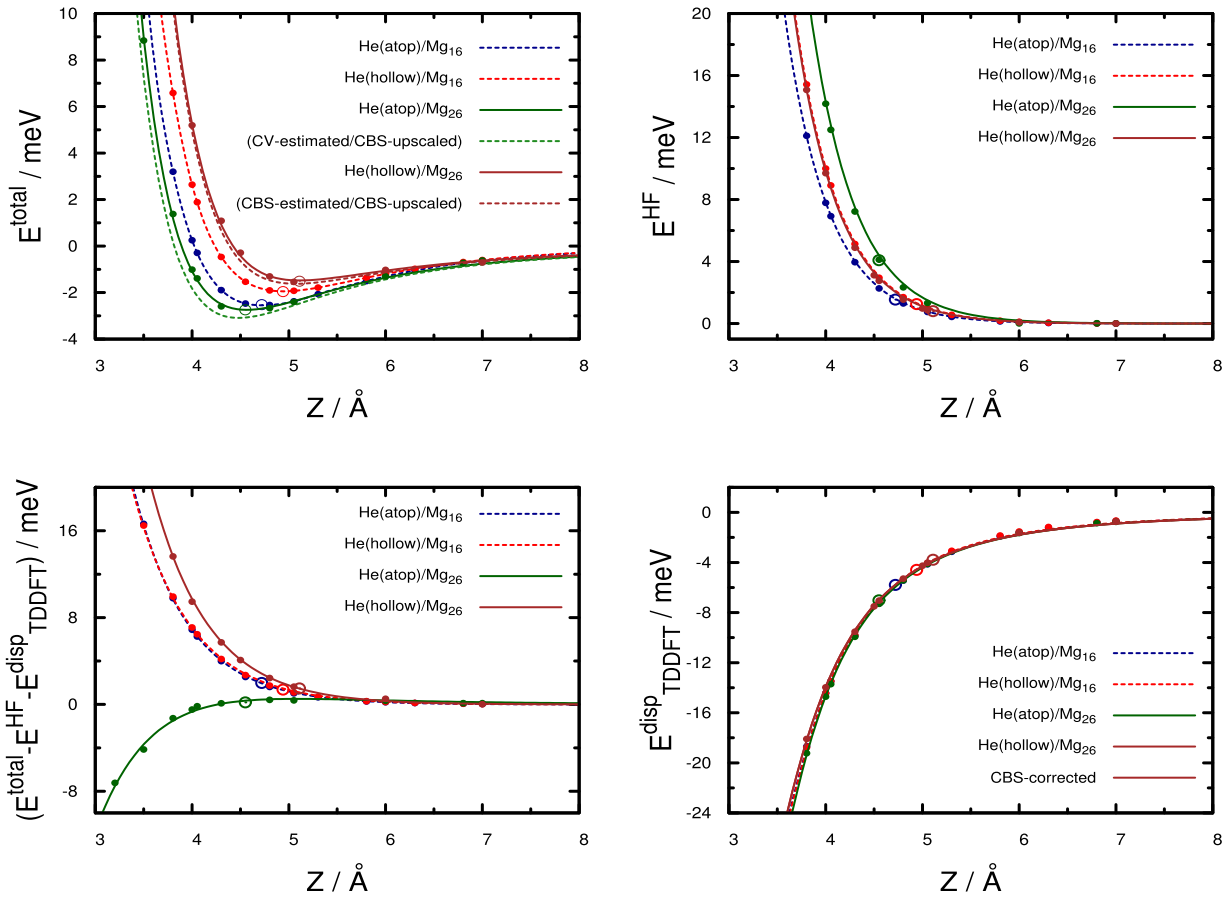

FIG. 4. Energy contributions to the He/Mg_{16} and the He/Mg_{26} interactions (see Eq. (1)) as a function of the He–cluster distance using the MP2C approach. The He atom is located at the "hollow" and "atop" adsorption sites (see Figure 1). The total interaction energies are fitted to the function $E^{total}(Z) = Ae^{-\alpha Z}Z^{\gamma} - C_3/(Z-d)^3$, from which the equilibrium distances have been determined.[61] Open circles indicate the values of the different energy terms at these distances, as listed in Table II.

However, dispersion terms such as the repulsive exchange-dispersion, and attractive ionic dispersion-like terms or those going beyond the dipole-dipole approximation are kept within this term at the uncoupled HF level using the MP2C approach.[20,21] The weight of the exchange-dispersion contribution is as high as 9% to the SAPT(PBE) dispersion energies at the shortest distances, decreasing rapidly at longer distances. Previous studies of the interaction of He atoms with non-metallic surfaces showed that the *intramonomer* correlation contribution is typically repulsive, decaying exponentially as the He-surface distance increases.[17,31] This can be interpreted in terms of the effect called "truncation of the correlation space" by Staemmler.[31] The contribution ($E_{int}^{tot} - E_{int}^{HF} - E_{TDDFT}^{disp}$) follows a purely exponential behaviour with the exception of the He("atop")/Mg_{26} system, for which a term going as $1/(Z-d)^5$ has been added to achieve a better fitting (see Figure 4). Hence, it cannot be concluded if the attractive nature of this contribution at short distances can be attributed either to an *intramonomer* correlation effect or to uncoupled HF dispersion-like terms left in the subtraction scheme (see Eq. (1)). The application of the method of increments at coupled-cluster level is more conclusive in this issue (see Sec. IV).

TABLE II. Decomposition of the He/Mg_{16} and the He/Mg_{26} interaction energies (see Eq. (1)) at the equilibrium distances (Z_e) for the "atop" and "hollow" configurations shown in Figure 1 (see also Figure 4).

	He/Mg_{16}		He/Mg_{26}	
	"atop"	"hollow"	"atop"	"hollow"
Z_e/Å	4.72	4.94	4.55	5.11
E_{int}^{total}/meV	−2.52	−1.96	−2.74	−1.51
E_{int}^{total} (CV-corrected)	−2.61	−2.01	−2.86	−1.55
E_{int}^{total} (CV-corrected/CBS-upscaled)	−2.73	−2.13	−3.08	−1.73
E_{int}^{HF}/meV	1.55	1.26	4.09	0.80
$(E_{int}^{tot} - E_{int}^{HF} - E_{TDDFT}^{disp})$/meV	1.98	1.37	0.19	1.47
E_{TDDFT}^{disp}/meV	−5.79	−4.59	−7.02	−3.78

The enhancement of the potential anti-corrugation upon increasing the metallic cluster size is interpreted as a signature of the appearance of screening effects when the He atom is located on-top of the Mg atom: the electronic density of the He atom would be screened by the metal through the density transfer to unoccupied $3p$ Mg orbitals. At this point, it is worth stressing that the cluster model might contain two complete hexagon-like shells of neighbors to the central Mg atom in the top-most layer, as well as the closest neighbors in the second and third layers, for this effect to show up. This mechanism might operate by transfer of the electrons from the $3p_z$ orbital of the central Mg atom to unoccupied orbitals of nearest and

next-nearest Mg atoms, in both the surface plane and deeper layers. This substrate-mediated charge-transfer mechanism would be less likely when the He atom is located at the "infinite-hollow" site due to the negligible overlap between the He 1*s* orbital and the Mg orbitals. It should be stressed that strong screening effects are clearly manifested in the similarity of the main dispersion (E^{disp}_{TDDFT}) contribution for the Mg_{26} and Mg_{16} clusters (see the lower-right panel of Fig. 4).

Concerning the uncertainty limit of our interaction energies, the SAPT(DFT)-based He/Mg_{16} binding energies are converged to within 0.16 meV (ca. 12%–17%) with respect to the estimated CBS limit. Similarly, the estimated core-valence correlation contributions and BSI corrections make the He/Mg_{26} global potential minimum about 0.34 meV deeper (ca. 11%). The benchmarking at CCSDT[51] and CCSDTQ[64] levels indicates that the MP2C approach performs remarkably well for the He–Mg pair, as shown in Figure S1 of the supplementary material.[64] As compared with CCSD(T) interaction energies,[64] the MP2C method underestimates the He/Mg_7 interaction by less than 7%.

To estimate the role of higher-order correlation corrections to the CCSD(T) treatment, CCSDT(Q) interaction energies have been calculated for the He/Mg_3 model system (i.e., including an iterative treatment of Q excitations). The Mg_3 cluster was composed by the central Mg atom and two of the six nearest neighbors shown in Fig. 1(c) and the He atom was located at the "hollow" configuration, with *Z* values ranging from 3.0 to 7.0 Å. As can be seen in Table S3 and Figure S3 of the supplementary material,[64] the largest energy difference between CCSD(T) and CCSDT(Q) interaction energies is found at the repulsive region: it amounts to 0.2 meV and about 8% of the corresponding well-depth value. Very recently, Martínez-Casado *et al.*[65,66] have shown that the estimate of higher-order corrections with the CCSDT(Q) method causes a decreasing of the He/MgO(100) binding energy by 1.1 meV (ca. 11% of the corresponding well-depth). For the He/Mg_3 system the perturbative treatment of triples excitations is the main responsible of the difference between CCSD(T) and CCSDT(Q) interaction energies and not the inclusion of perturbative quadruple excitations. Thus, the CCSDT and CCSDT(Q) interaction energies differs by less than 0.03 meV (ca. 1.6%) and these energy differences are very similar when considering two different basis sets for the Mg atom.[64] Further work using larger He/Mg_n models is necessary to quantify high-order correlation corrections for the He/Mg(0001) interaction beyond the CCSD(T) approach.

As demonstrated by Shepherd and Grüneis,[62] the MP2 method and the perturbative triples (T) treatment within the CCSD(T) approach diverges when applied to the homogeneous electron gas. A divergence of the (T) term has also been shown in previous CCSD(T) studies of bulk Ca and Sr using the method of increments.[34] Thus, the (T) contribution increased the correlation energy by about 30%, reflecting the strong multi-reference character of the wave-function. In contrast, the (T) term accounted for less than 11% of the correlation energy for bulk Mg, as also found for the He/Mg(0001) system in the present work. Hence, the divergence signal of the homogeneous electron gas is not manifested in our cluster-based calculations despite of the Mg metallic character. It would be very interesting to apply the scheme proposed by Shepherd and Grüneis[62] in larger He/Mg_n systems than those addressed in this work, by using the Thomas-Fermi screened Coulomb operator in the calculation of the MP2 amplitudes.[62] Nonetheless, considering that the main dispersion contribution to the He/Mg_n interaction is almost "saturated" with $n = 26$, we do not expect qualitative differences when the number of Mg atoms is further increased. Consistently, the MP2C-based He/Mg_{26} interaction energies are rather similar to those evaluated at CCSD(T) level in embedded Mg_n clusters (see Sec. IV).

IV. ANALYSIS OF THE HE/MG(0001) INTERACTION VIA THE METHOD OF INCREMENTS

As mentioned above, the application of the method of increments allows to dissect the correlation contributions to the interaction in *intramonomer* and (dispersion-like) *intermonomer* terms (see Eq. (2)). As applied in this work, it has enabled the breakdown of these correlation terms in one-, two-, and three-body contributions. Figure 5 shows the dependence of the different energy contributions on the He–Mg(0001) distance. Confirming the analysis from MP2C calculations on unembedded clusters (see Sec. III B), the "atop" configuration is more stable due to the more attractive *intramonomer* correlation contributions (see left panel of Figure 5). As first found for the Xe/Mg(0001) system,[8] the attractive nature of the two-body *intramonomer* correlation term for the "atop" geometry is mostly responsible for this behaviour (right panel of Figure 5). In contrast, this contribution is repulsive when the adsorbate is located at the "infinite-hollow" site, as found for the adsorbate on non-metallic surfaces (see, e.g., Refs. 16 and 18). As discussed in Ref. 8, the attractive nature of the *intramonomer* correlation contribution reflects that the perturbation of the adsorbate is effectively screened by the metal when the adsorbate approaches the "atop" surface site. The magnitude of this contribution decays exponentially as the He-surface distance increases, as typically found for *intramonomer* correlation terms[17,31] but bearing the opposite sign.

The dispersion-like *intermonomer* correlation contribution is clearly dominated by two-body incremental terms, being also slightly more attractive for the "atop" configuration. Table III provides a detailed breakdown of the periodic HF and incremental energy contributions at the potential minima for "atop" and "hollow" structures. Notice that the metal screening for the "atop" geometry allows a closer approach of the He atom to the surface so that the equilibrium distance is ca. 0.6 Å shorter. Subsequently, the dispersion-like *intermonomer* correlation contribution is about a factor of 1.6 larger at the "atop" potential minimum. We notice that the three-body dispersion-like contributions are attractive, as opposed to non-metallic surfaces,[16,18] accounting for ca. 9% of the total dispersion in the well region. From Table III, it can be also noticed the very small magnitude of the most relevant *intramonomer* three-body and *intermonomer* four-body increments, as compared with

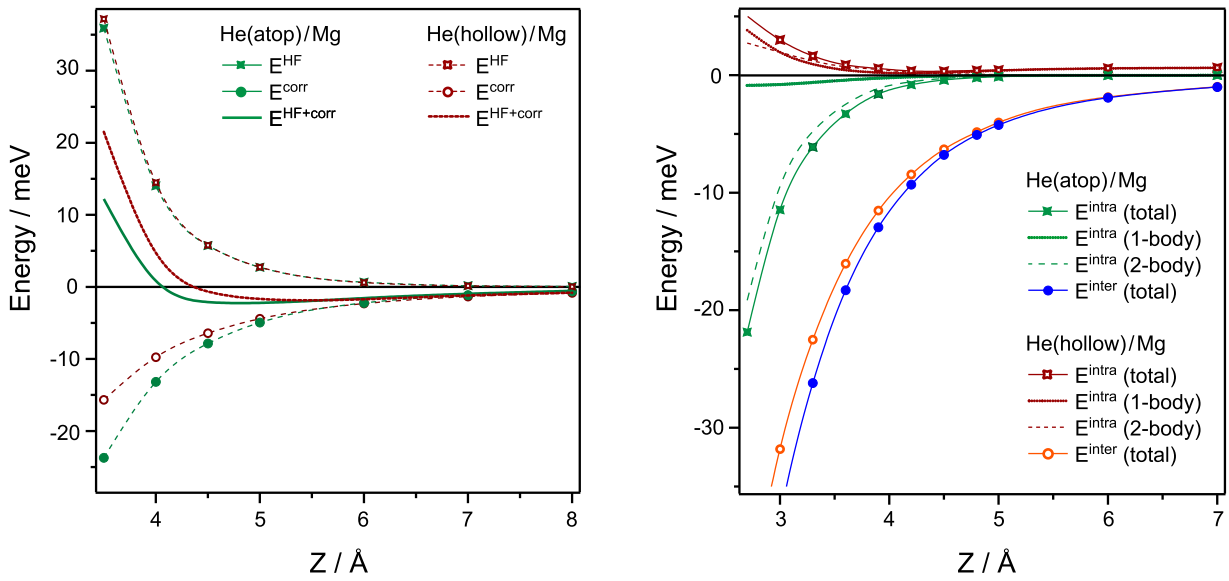

FIG. 5. Energy contributions to the He/Mg(0001) interaction as functions of the adsorbate-surface distance evaluated with the method of increments for the two considered adsorption configurations.

TABLE III. Decomposition of the He/Mg(0001) interaction energy (in meV) using the method of increments at the calculated equilibrium distances for "atop" ($Z_e = 4.8$ Å) and "hollow" ($Z_e = 5.4$ Å) configurations. CBS-upscaled and CV-corrected total energies are also tabulated.[63,64] The breakdown of *intramonomer* and *intermonomer* correlation contributions in n-body increments is specified (see Eqs. (3) and (4)). The values of the most relevant two- and higher-order increments are also shown. The contribution of successive deeper layers to the total two-body *intermonomer* correlation term is also indicated (see the supplementary material for the incremental contributions at different He-surface distances[64]).

	"atop"	"hollow"
Z_e/Å	4.8	5.4
E_{int}^{total}	−2.55	−1.94
E_{int}^{total} (CBS-upscaled)	−3.21	−2.42
E_{int}^{total} (CBS-upscaled/CV-corrected)	−3.24	−2.42
E_{int}^{HF}	3.46	1.27
E_{int}^{intra} (total)	−0.18	0.51
E_{int}^{inter} (total)	−5.83	−3.72
	E_{int}^{intra} (total)	
$\sum\eta_i + \eta_A$ (1-body)	−0.05	0.50
$\sum\eta_{ij}$ (2-body)	−0.14	0.01
η_{ij} (2-body)	−0.014	0.006
η_{ijk} (3-body)	−0.002	0.001
	E_{int}^{inter} (total)	
$\sum\eta_{Ai}$ (2-body)	−5.35	−3.41
$\sum\eta_{Aij}$ (3-body)	−0.48	−0.31
η_{Ai} (2-body)	−1.058	−0.358
η_{Aij} (3-body)	0.077	0.020
η_{Aijk} (4-body)	0.003	0.002
	E_{int}^{inter} (2-body)	
$\sum\eta_{Ai}$, $i \in$ (S)	−4.42	−2.86
$\sum\eta_{Ai}$, $i \in$ (S-1)	−0.90	−0.56
$\sum\eta_{Ai}$, $i \in$ (S-2)	−0.03	−0.01

the two-body and three-body counterparts. It reflects that the n-body incremental expansion is well converged by considering up to two-body *intramonomer* and three-body *intermonomer* increments. For shorter He-surface distances (see the supplementary material[64]), the three-body dispersion contribution is kept attractive for the "atop" configuration, becoming repulsive for the "hollow" geometry instead. Similarly to the *intramonomer* two-body correlation term, this opposite behaviour might stem from the screening of the adsorbate perturbation by redistribution of the metal electronic density for the "atop" geometry. Interestingly, that redistribution causes an effectively more attractive interaction between surface fluctuating dipoles. Once again, incremental three-body terms have been found to be repulsive for atomic helium on non-metallic surfaces[16,18] and this behaviour has been explained by considering the screening in the interaction between fluctuating dipoles located at two substrate atoms by the adsorbate.[19]

Let us now analyze the weighting of successively deeper Mg(0001) surface layers to the total two-body dispersion-like contribution (three last rows of Table III). The dispersion contribution results mainly from the adsorbate interaction with the top-most surface layer, accounting for ca. 83%–84% of the total two-body dispersion-like term. The second surface layer is mostly responsible for the remaining *intermonomer* correlation term while the third layer contribution is insignificant (less than 1%). The weighting is very similar for different He-surface separations.[64] As also revealed by applying the MP2C treatment (see Sec. III B), this behaviour essentially results from the screening exerted by the top-most Mg atoms in those located in deeper layers, being almost complete for atoms in the third layer. By comparing Tables II and III, it can be noticed that the MP2C-based well-depth values agree rather well with those determined with the method of increments (to within 0.5 meV). The consistency between the two schemes is also reflected in

the very similar estimate of the laterally average dispersion interaction (see Sec. V C).

V. THE ADDITIVE PAIRWISE POTENTIAL MODEL

An additive pairwise potential model has been employed to fit the Hartree-Fock and the correlation contributions to the interaction energy, as obtained with the method of increments. Pairwise potential models exploiting energy partition schemes have been previously proposed for the argon interaction with gold surfaces.[67] The model proposed in this work can be viewed as an extended version of the modified Lennard-Jones functional developed by Carlos and Cole,[68,69] to account for corrugation effects in the interaction between noble-gases and the graphite surface.

A. Pairwise additive model for the Hartree-Fock contribution

The repulsive Hartree-Fock interaction energies were fitted to the pairwise additive functional,

$$E_{\rm int}^{\rm HF}(\{\mathbf{R}_{\rm HeMg}\}) = \sum_{\rm Mg}[1+\gamma_R(1-\frac{6}{5}\cos^2\theta_{\rm Mg})] \times A\, e^{(-\alpha\, R_{\rm HeMg}-\beta\, R_{\rm HeMg}^2)} \quad R_{\rm HeMg} < R_c$$
$$= 0, \qquad R_{\rm HeMg} > R_c, \qquad (5)$$

where $R_{\rm HeMg}$ stands for the distance between the He atom and one surface Mg atom, $\theta_{\rm Mg}$ is the angle between the surface normal and the vector $\mathbf{R}_{\rm HeMg}$ from the noble-gas atom to the same Mg atom, and R_c is a cutoff distance. Notice that the dimensionless factor γ_R in the first term modulates the corrugation amplitude. For anti-corrugated cases, the interaction energy is less repulsive directly above the surface Mg atoms, with $\cos^2\theta_{\rm Mg}$ adopting a value close to unity. This is translated in positive γ_R values. The opposite holds when the interaction energy becomes less repulsive for the noble-gas atoms adsorbed on "hollow" sites. This is the case of the graphite surface, for which a γ_R value of −0.54 has been reported.[68,69] Table IV lists the PPM parameters for the repulsive contribution. A modest anti-corrugation is reflected in the positive value of the γ_R parameter (1.37) which can be compared with the (negative) value for the He/graphite interaction (−0.54 from Ref. 68).

B. Pairwise additive model for correlation contribution

The total correlation energy contribution was fitted by means of the D_{as} functional of Szalewicz and collaborators,[71–73] but modulated by a corrugation scaling factor,

$$E_{\rm int}^{\rm corr}(\{\mathbf{R}_{\rm HeMg}\}) = -\sum_{\rm Mg}[1+\gamma_A(1-\frac{3}{2}\cos^2\theta_{\rm Mg})] \times \sum_{n=6,8}\frac{\sqrt{C_n^{\rm He}C_n^{\rm Mg}}}{R_{\rm HeMg}^n} f_n\left(\sqrt{\beta_{\rm He}\beta_{\rm Mg}}R_{\rm HeMg}\right), \qquad (6)$$

TABLE IV. Parameters defining the Hartree-Fock, total correlation, and *intermonomer* correlation contributions to the He/Mg(0001) interaction energy using the pairwise additive potential model proposed in this work. The parameters were obtained from the interaction energies evaluated with the method of increments (cf. text). The values of the $C_6^{\rm He}$, $C_8^{\rm He}$, and $\beta^{\rm He}$ parameters were fixed to those reported by Podeszwa *et al.*[73] Z is assumed in Å.

Hartree-Fock interaction energy				
R_c/Å	A/eV	α/Å^{-1}	β/Å^{-2}	γ_R
18.0	131.474	2.708	−0.756	1.37
Total correlation energy contribution				
	C_6^X/eV Å^6	C_8^X/eV Å^8	β^X/Å^{-1}	γ_A
X = Mg	83.268	2731.39	1.583	−7.53
***Intermonomer* correlation energy contribution**				
X = Mg	192.51	1701.66	1.712	−0.33
X = He	0.678	5.493	4.377	...

where the sum in the second term (the D_{as} function) runs over as many surface Mg atoms as necessary to get convergence and f_n are the damping functions of Tang and Toennies.[74] Once again, notice that the dimensionless factor γ_A in the first term measures the anti-corrugation strength, with γ_A bearing a negative value. For comparison purposes, Table IV also list the parameters obtained upon the separate fitting of the *intermonomer* correlation contribution.

When fitting the CCSD(T) correlation contributions for the "atop" and "hollow" configurations, all one-, two-, and three-body incremental terms were considered. Table IV lists the values of the parameters along with the anisotropic γ_A factor. Notice that the value of γ_A is negative (−7.53) and relatively very large when compared to its repulsive Hartree-Fock counterpart (i.e., γ_R = 1.37). It highlights that the anti-corrugation is mainly an electronic correlation effect. More precisely, the very small γ_R value obtained when the *intermonomer* correlation term is fitted separately (i.e., γ_R = −0.33) demonstrate that the short-range *intramonomer* correlation contribution is mostly responsible of the potential anti-corrugation. In fact, the anti-corrugation in the vdW *tail* is very weak as compared with that characterizing the potential wall.

Figure 6 presents the PPM interaction potentials. For comparison purposes, the potential energy curves evaluated with the PBE-D2 treatment and the pairwise addition of He–Mg potentials[75,76] are also shown. What it is important to note is that the PPM provides an excellent representation of both the strength and the anisotropy of interaction at the repulsive potential region, providing also accurate vdW long-range *tails*. However, the PPM underestimates the anisotropy of the interaction at the minima potential region, where the interaction energy is about 0.15 meV less attractive/repulsive for "atop"/"hollow" structures. This deficiency could arise from the lack of three-body He-Mg_2 terms in the PPM. Nonetheless, the energy differences are within the uncertainty limits of the CCSD(T) interaction energies themselves. Thus, the estimated correction for CV correlation and the BSI effect amounts to 0.7 meV in global potential minimum (see Table III). The fine-tuning of the PPM parameters might also

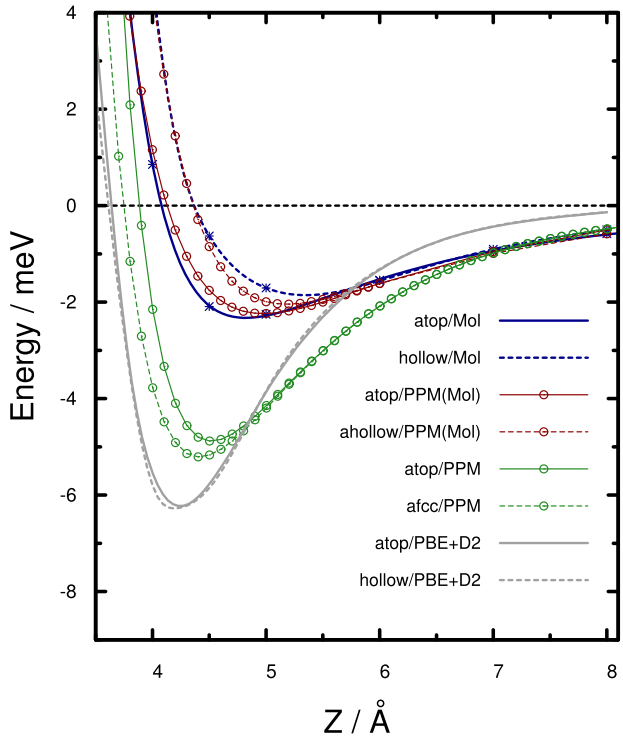

FIG. 6. He/Mg(0001) interaction energies as functions of the distance Z as obtained with the method of increments (referred to as "MoI" in the figure), the PBE-D2 approach, and our pairwise potential model, with the parameters extracted from incremental calculations (denoted as (PPM/MoI) in the figure). The potential energy curves obtained by the pairwise addition of He–Mg potentials[75,76] (termed PPM in the figure) are also represented (cf. text).

consider additional adsorption sites. The improvement of the PPM itself would likely be possible by considering diatomic surface fragments as the building blocks.[70]

Focusing on the PBE-D2 interaction potential shown in Figure 6, it can be noticed that it is too attractive, as found in other He/surface systems.[16–19] A localized molecular orbital decomposition energy analysis indicated that the PBE approach underestimates the repulsive *intramonomer* correlation contribution to the He/TiO_2(110) interaction,[17] causing overbinding effects when adding the dispersion correction. Our present results indicate that the PBE functional provides very similar interaction energies at different adsorption sites so that the resulting PBE-D2 potential is almost no corrugated. One possible explanation is that the PBE electronic densities are too delocalized and isotropic for the corrugation being proved by the small spherical-like He atom. Thus, the PBE-D2 approach performs well in describing the Xe/Mg(0001) interaction.[8] Considering a graphene surface, it has been shown that the overall performance of vdW-corrected DFT approaches improves as the size of the adsorbed noble-gas atom increases while the dispersion tail is reasonably well described by means of the vdW correction for all noble-gas atoms.[19]

For the sake of comparison, Figure 6 also shows the potential energy curves obtained as a sum of pairwise He–Mg potentials. We used the He–Mg interaction potential calculated by Mella *et al.*[75] at CCSD(T) level, and parametrized by Navarro *et al.*[76] From Figure 6, it can be seen that the standard additive pairwise approximation reproduces very well the long-range tails. However, an opposite potential corrugation is predicted with the "hollow" site being more attractive, and also potential minima which are about a factor of 2.5 deeper. This indicates that dynamical simulations of the synthesis of Mg nanoparticles within He nanodroplets might consider pairwise potential models beyond the standard pairwise approximation. In contrast, Mella *et al.*[75] have demonstrated that the pairwise approximation is very reliable for the interaction of one Mg atom with He_n clusters as a sum of n He–Mg interactions. Despite of the underestimation of the potential anisotropy at the potential minima, our proposed model may represent a significant improvement over the standard approximation. Aimed to adapt it to the interaction of He with Mg_n clusters, an orientational average of the pairwise potential would be necessary due to lack of a well-defined surface.

TABLE V. Well-depth D_{min}, equilibrium distance Z_{min}, and dispersion coefficient C_3 characterizing the He/Mg(0001) and the He/Mg(111) LAPs.[77,78] The value in parenthesis has been extracted from the PPM applied to the MP2C dispersion contribution E_{disp}^{TDDFT} in the He/Mg_{26} interaction. Values between brackets encompasses an estimate of BSI effects.[63]

	Z_{min}/meV	D_{min}/Å	C_3/meV Å^3
PPM	5.12	−2.13	147 (145)
	[4.97]	[−2.35]	[159]
Reference[a]	5.04	−2.77	153

[a]Values of Ref. 77.

C. Laterally average potential

Aimed to compare directly with the laterally average interaction of He with a *fcc* Mg(111) surface,[13,14,77] we have determined the laterally average potential (LAP) for the He/Mg(0001) interaction. For this purpose, interaction energies were evaluated by applying our pairwise potential model into an evenly space XY grid of 100×100 positions. Table V collects the main parameters characterizing the LAPs. It can be noticed that the He/Mg(0001) LAP is slightly less attractive than the counterpart in the *fcc* Mg(111) surface. This is consistent with the fact that the Mg(111) surface, with a face-centered cubic (*fcc*) structure, lacks of the less attractive "infinite-hollow" *fcc* sites. Notice also that the dispersion C_3 coefficients bear very similar values to each other, including that extracted from the He/Mg_{26} (TDDFT-based) dispersion energies.

VI. SUMMARY AND CONCLUDING REMARKS

Summarizing, two different post-Hartree-Fock approaches provide clear evidences of the anti-corrugated nature of the He/Mg(0001) potential, with the "infinite-hollow" sites being more repulsive at short distances and less attractive at the long-range potential region. As previously discussed for the Xe/Mg(0001) interaction,[8] *intramonomer* correlation contributions are found to be responsible for the more attractive interaction when the He atom is located directly above one Mg surface atom. The enhancement of the

anti-corrugation effect upon increasing the size of the cluster modeling the Mg(0001) surface is also evidenced. The more attractive interaction for the He atom at the "atop" structure is interpreted as a screening effect through the transfer of the electronic density from the adsorption region to regions lying both in the parallel and perpendicular orientations to the surface plane. The variation of the metal cluster composition makes clear that the Mg atom directly beyond the adatom must be surrounded by two complete Mg "solvation shells" for the anti-corrugation signal to be enhanced.

The breakdown of the *intramonomer* correlation contributions provided by the method of increments indicates that attractive two-body incremental terms are mostly responsible for the anti-corrugation feature. The strong screening in the metal surface is also reflected in the relative contribution of successively deeper Mg(0001) layers to the main dispersion contribution, being insignificant for the third layer. Although the He/surface *intermonomer* correlation contribution is dominated by two-body terms, the three-body increments represent a significant (attractive) portion (ca. 9% at the potential minima). At a variance, previous studies of the interaction of atomic helium with non-metallic surfaces indicated that three-body terms cause an effective reduction of the dispersion contribution.[16–19] Also in marked contrast, no corrugation is found when the density functional PBE has been applied, including a dispersion correction.

We have also developed a potential model for the He/Mg(0001) interaction based on the pairwise additive sum of He–Mg potential functions. As variables, the functions depend on both the He–Mg distance (R_{HeMg}) and the angle between the $\mathbf{R}_{HeMg}$ vector and the surface normal. The repulsive potential region and the long-range tails are remarkably well described by the potential model while the anisotropy at the potential minima region is underestimated. The pairwise sum of the potentials obtained for the isolated He–Mg system leads to a too attractive interaction (by a factor of ca. 2.5) and opposite corrugation features. The laterally averaged He/Mg(0001) potential resulting from our potential model agrees well with that determined for the *fcc* Mg(111) surface by Zaremba and Konh,[14] taking into account the lack of infinite "hollow" sites in the latter. Work is in progress to adapt our potential model for dynamical studies addressing the He droplet-mediated synthesis of metallic nanoparticles.[79] The application of advanced vdW-DFT treatments is envisaged, incorporating improvements that enable an even more accurate *ab initio* benchmarking. These include more precise extrapolation schemes to the complete basis set limit and advanced protocols to estimate high-order correlation corrections in the coupled-cluster treatment, as well as the application of the screened MP2 method[62] in larger He/Mg_n systems.

ACKNOWLEDGMENTS

This work has been partly supported by the COST Action No. CM1405 "Molecules in Motion (MOLIM)," Grant Nos. FIS2011-29596-C02-01 and MAT2012-33633 from the Spanish Dirección General de Investigación Científica y Técnica, and the German Research Foundation (DFG) through Project No. VO 1711/2-1. The Cesga Super-Computer Center (Galicia), and the Centro Técnico de Informática (CTI, CSIC) are acknowledged for allocating computer time.

[1] J. L. F. Da Silva, C. Stampfl, and M. Scheffler, Phys. Rev. Lett. **90**, 066104 (2003).
[2] T. Seyller, M. Caragiu, R. D. Diehl, P. Kaukasoina, and M. Lindroos, Phys. Rev. B **60**, 11084 (1999).
[3] P. Thomas, J. Gray, X. D. Zhu, and C. Y. Fong, Chem. Phys. Lett. **381**, 376 (2003).
[4] J. F. Annett and R. Haydock, Phys. Rev. Lett. **53**, 838 (1984).
[5] J. F. Annett and R. Haydock, Phys. Rev. Lett. **57**, 1382 (1986).
[6] K. H. Rieder, G. Parschau, and B. Burg, Phys. Rev. Lett. **71**, 1059 (1993).
[7] J. Harris and E. Zaremba, Phys. Rev. Lett. **55**, 1940 (1985).
[8] E. Voloshina, Phys. Rev. B **85**, 045444 (2012).
[9] Y. N. Zhang, V. Bortolani, and G. Mistura, Phys. Rev. B **89**, 165414 (2014).
[10] M. Alcántara Ortigoza, M. Aminpour, and T. S. Rahman, Phys. Rev. B **91**, 115401 (2015).
[11] M. Dion, H. Rydberg, E. Schröder, D. C. Langreth, and B. I. Lundqvist, Phys. Rev. Lett. **92**, 246401 (2004).
[12] K. Lee, E. Eamonn, L. Kong, B. I. Lundqvist, and D. C. Langreth, Phys. Rev. B **82**, 081101(R) (2010).
[13] E. Zaremba and W. Kohn, Phys. Rev. B **13**, 2270 (1976).
[14] E. Zaremba and W. Kohn, Phys. Rev. B **15**, 1769 (1977).
[15] A. Michaelides, T. J. Martinez, A. Alavi, G. Kresse, and F. R. Manby, J. Chem. Phys. **143**, 102601 (2015).
[16] M. P. de Lara-Castells, H. Stoll, B. Civalleri, M. Causá, E. Voloshina, A. O. Mitrushchenkov, and M. Pi, J. Chem. Phys. **141**, 151102 (2014).
[17] M. P. de Lara-Castells, H. Stoll, and A. O. Mitrushchenkov, J. Phys. Chem. A **118**, 6367 (2014).
[18] M. P. de Lara-Castells, N. F. Aguirre, H. Stoll, A. O. Mitrushchenkov, D. Mateo, and M. Pi, J. Chem. Phys. **142**, 131101 (2015).
[19] M. P. de Lara-Castells, M. Bartolomei, A. O. Mitrushchenkov, and H. Stoll, J. Chem. Phys. **143**, 194701 (2015).
[20] A. Heßelmann, J. Chem. Phys. **128**, 144112 (2008).
[21] M. Pitonák and A. Heßelmann, J. Chem. Theory Comput. **6**, 168 (2010).
[22] F. Della Sala and A. Görling, J. Chem. Phys. **115**, 5718 (2001).
[23] M. Bartolomei, E. Carmona-Novillo, M. I. Hernández, J. Campos-Martínez, and F. Pirani, J. Phys. Chem. C **117**, 10512 (2013).
[24] M. P. de Lara-Castells, A. O. Mitrushchenkov, and H. Stoll, J. Chem. Phys. **143**, 102804 (2015).
[25] A. J. Misquitta, B. Jeziorski, and K. Szalewicz, Phys. Rev. Lett. **91**, 033201 (2003).
[26] A. Heßelmann and G. Jansen, Chem. Phys. Lett. **367**, 778 (2003).
[27] H. Stoll, Phys. Rev. B **46**, 6700 (1992).
[28] H. Stoll, J. Chem. Phys. **97**, 8449 (1992).
[29] C. Müller and B. Paulus, Phys. Chem. Chem. Phys. **14**, 7605 (2012).
[30] L. Hammerschmidt, L. Maschio, C. Müller, and B. Paulus, J. Chem. Theory Comput. **11**, 252 (2015).
[31] V. Staemmler, J. Phys. Chem. A **115**, 7153 (2011).
[32] E. Voloshina, D. Usvyat, M. Schütz, Y. Dedkov, and B. Paulus, Phys. Chem. Chem. Phys. **13**, 12041 (2011).
[33] E. Voloshina, N. Gaston, and B. Paulus, J. Chem. Phys. **126**, 134115 (2007).
[34] E. Voloshina and B. Paulus, J. Chem. Theory Comput. **10**, 1698 (2014).
[35] V. Mozhayskiy, M. N. Slipchenko, V. K. Adamchuk, and A. F. Vilesov, J. Chem. Phys. **127**, 094701 (2007).
[36] L. F. Gómez, E. Loginov, and A. F. Vilesov, Phys. Rev. Lett. **108**, 155302 (2012).
[37] G. Haberfehlner, P. Thaler, D. Knez, A. Volk, F. Hofer, W. E. Ernst, and G. Kothleitner, Nat. Commun. **6**, 8779 (2015).
[38] P. Thaler, A. Volk, F. Lackner, J. Steurer, D. Knez, W. Grogger, F. Hofer, and W. E. Ernst, Phys. Rev. B **90**, 155442 (2014).
[39] D. Spence, E. Latimer, C. Feng, A. Boatwright, A. Ellis, and S. Yang, Phys. Chem. Chem. Phys. **16**, 6903 (2014).
[40] S. B. Emery, K. B. Rider, and C. M. Lindsay, Propellants, Explos., Pyrotech. **39**, 161 (2014).
[41] S. B. Emery, Y. Xin, C. J. Ridge, R. J. Buszek, J. A. Boatz, J. M. Boyle, B. K. Little, and C. M. Lindsay, J. Chem. Phys. **142**, 084307 (2015).
[42] R. A. Varin, T. Czujko, and Z. S. Wronski, *Nanomaterials for Solid State Hydrogen Storage* (Springer, New York, 2009).
[43] A. Zaluska, L. Zaluski, and J. O. Ström-Olsen, J. Alloys Compd. **288**, 217 (1999).
[44] A. Heßelmann, G. Jansen, and M. Schütz, J. Chem. Phys. **122**, 014103 (2005).

[45]B. Jeziorski, R. Mozynski, A. Ratkiewicz, S. Rybak, K. Szalewicz, and H. L. Williams, in *Methods and Techniques in Computational Chemistry,* Volume B: Medium Size Systems, edited by E. Clementi, METECC94 (D. Reidel Publishing Company, STEF, Cagliari, 1993), p. 79.
[46]J. P. Perdew, K. Burke, and M. Ernzerhof, Phys. Rev. Lett. **77**, 3865 (1996).
[47]S. Grimme, J. Comput. Chem. **27**, 1787 (2006).
[48]H.-J. Werner, P. J. Knowles, G. Knizia, F. R. Manby, M. Schütz *et al.*, MOLPRO, version 2012.1, a package of *ab initio* programs, 2012, see http://www.molpro.net.
[49]D. E. Woon and T. H. Dunning, Jr., J. Chem. Phys. **100**, 2975 (1994).
[50]K. A. Peterson and T. H. Dunning, J. Chem. Phys. **117**, 10548 (2002).
[51]R. J. Hinde, J. Phys. B: At. Mol. Opt. Phys. **35**, 3119 (2003).
[52]MRCC, a quantum chemical program suite written by M. Kállay, Z. Rolik, J. Csontos, I. Ladjánszki, L. Szegedy, B. Ladóczki, and G. Samu. See also Z. Rolik, L. Szegedy, I. Ladjánszki, B. Ladóczki, and M. Kállay, J. Chem. Phys. **139**, 094105 (2013), as well as www.mrcc.hu.
[53]M. Kállay and P. Surján, J. Chem. Phys. **115**, 2945 (2001).
[54]M. Grüning, O. V. Gritsenko, S. V. A. van Gisbergen, and E. J. Baerends, J. Chem. Phys. **114**, 652 (2001).
[55]S. G. Lias, "Ionization energy evaluation," in NIST Chemistry Web-Book, NIST Standard Reference Database No. 69, 2016, http://webbook.nist.gov.
[56]T. Helgaker, W. Klopper, H. Koch, and J. Noga, J. Chem. Phys. **106**, 9639 (1997).
[57]S. F. Boys and F. Bernardi, Mol. Phys. **19**, 553 (1970).
[58]P. Fuentealba, L. von Szentpaly, H. Preuss, and H. Stoll, J. Phys. B **18**, 1287 (1985).
[59]R. Dovesi, R. Orlando, A. Erba, C. M. Zicovich-Wilson, B. Civalleri, S. Casassa, L. Maschio, M. Ferrabone, M. De La Pierre, P. D'Arco, Y. Noël, M. Causá, M. Rérat, and B. Kirtman, Int. J. Quantum Chem. **114**, 1287 (2014).
[60]R. Dovesi, V. R. Saunderds, C. Roetti, R. Orlando, C. M. Zicovich-Wilson, F. Pascale, B. Civalleri, K. Doll, N. M. Harrison, I. J. Bush, P. D'Arco, M. Llunel, M. Causá, and Y. Noël, *CRYSTAL14 User's Manual* (Universitá Torino, Torino, 2014), http://www.crystal.unito.it.
[61]The dispersion energy terms E^{disp}_{TDDFT} in Fig. 4 have been fitted to the function $\sum_n -C_n/(Z-d)^n$ (n = 3, 5, 7) while the exponential function $A\, e^{-\alpha\, Z}$ has been used for the repulsive (e.g., Hartree-Fock) energy contributions. The attractive energy term ($E^{total} - E^{HF} - E^{disp}_{TDDFT}$) is fitted to the function $-A\, e^{-\alpha\, Z} + C_5/(Z-d)^5$.
[62]J. J. Shepherd and A. Grüneis, Phys. Rev. Lett. **110**, 226401 (2013).
[63]The f_{CBS} upscaling factors were calculated at CCSD(T) level for "atop" and "hollow" He/Mg_7 structures, using aug-cc-pVTZ and aug-cc-pVQZ basis sets. Values of 1.11 and 1.15 were determined at the potential minima.
[64]See supplementary material at http://dx.doi.org/10.1063/1.4954772 for the assessment of the performance of the MP2C method in the Mg–He interaction, the estimation of core-valence correlation contributions to the He/Mg_n interaction ($n < 8$) at CCSD(T) level, the detailed breakdown of the correlation energy terms calculated with the method of increments at different He-surface distance, and the He/Mg_3 interaction energy at CCSDT(Q) level.
[65]R. Martinez-Casado, D. Usvyat, G. Mallia, L. Maschio, S. Casassa, J. Ellis, M. Schütz, and N. M. Harrison, Phys. Chem. Chem. Phys. **16**, 21106 (2014).
[66]R. Martinez-Casado, D. Usvyat, L. Maschio, G. Mallia, S. Casassa, J. Ellis, M. Schütz, and N. M. Harrison, Phys. Rev. B **89**, 205138 (2014).
[67]R. Grenier, Q.-D. To, M. P. de Lara-Castells, and C. Leonard, J. Phys. Chem. A **119**, 6897 (2015).
[68]W. E. Carlos and M. W. Cole, Surf. Sci. **91**, 339 (1980).
[69]L. W. Brunch, M. C. Cole, and E. Zaremba, *Physical Adsorption: Forces and Phenomena* (Clarendon Press, Oxford, 1997).
[70]R. Hatz, M. Korpinen, V. Hänninen, and L. Halonen, J. Phys. Chem. A **119**, 11729 (2015).
[71]K. Pernal, R. Podeszwa, K. Patkowski, and K. Szalewicz, Phys. Rev. Lett. **103**, 263201 (2009).
[72]R. Podeszwa and K. Szalewicz, J. Chem. Phys. **136**, 161102 (2012).
[73]R. Podeszwa, K. Pernal, K. Patkowski, and K. Szalewicz, J. Phys. Chem. Lett. **1**, 550 (2010).
[74]K. T. Tang and J. P. Toennies, J. Chem. Phys. **80**, 3726 (1984).
[75]M. Mella, G. Calderoni, and F. Cargnoni, J. Chem. Phys. **123**, 054328 (2005).
[76]J. Navarro, D. Mateo, M. Barranco, and A. Sarsa, J. Chem. Phys. **136**, 054301 (2012).
[77]G. Vidali, G. Ihn, H.-Y. Kim, and M. W. Cole, Surf. Sci. Rep. **12**, 133 (1991).
[78]The long-range tail of the LAP was fitted to the function $-C_3/(Z-d)^3$, with the d value fixed to that tabulated in Ref. 73.
[79]A. W. Hauser, A. Volk, P. Thaler, and W. E. Ernst, Phys. Chem. Chem. Phys. **17**, 10805 (2015).